machines

MDPI

Article

Reproduction of Road Scenarios for Simulated Driving Using LiDar Surveying Technique

Roberta Finelli [1], Pasquale Sena [2], Angelo Lorusso [1], Liliana Cecere [1] and Francesco Villecco [1,*]

[1] Department of Industrial Engineering, University of Salerno, Via Giovanni Paolo II, 132, 84084 Fisciano, Italy; r.finelli4@studenti.unisa.it (R.F.); alorusso@unisa.it (A.L.); lcecere@unisa.it (L.C.)
[2] Department of Pharmacy, University of Salerno, Via Giovanni Paolo II, 132, 84084 Fisciano, Italy; psena@unisa.it
* Correspondence: fvillecco@unisa.it; Tel.: +39-089-964324

Abstract: Nowadays, driving simulation devices represent a continuously evolving and developing area in the world of virtual reality. One of the fundamental elements in the design of driving software is the track model. This work aims to study the use of advanced technologies for the three-dimensional modeling of a racing track in a driving simulator. Specifically, it employs the LiDAR methodology to acquire the three-dimensional coordinates of a 1 km long circuit located on the Fisciano campus of the University of Salerno. The purpose of this work is to explain and present a novel track acquisition and modeling methodology within the realm of simulated driving reality. Following the study, the Virtual Reality Laboratory's driving simulator at the Department of Industrial Engineering conducted tests to validate the proposed circuit model. The test rides analyzed the realism of the driving experience, thereby validating the proposed track model. This phase was complemented by a series of proposals for possible future developments in the field of three-dimensional modeling applied to driving simulation and beyond. In the end, the 3D model obtained demonstrated the high definition of the acquired result and the speed with which multiple data were obtained simultaneously, thanks to the laser scanner used.

Keywords: driving simulation; LiDAR data; 3D modeling; virtual reality; track modeling; real-world driving; virtual environment; virtual reality

check for updates

Academic Editor: Xiang Li

Received: 20 November 2024
Revised: 12 December 2024
Accepted: 18 December 2024
Published: 25 December 2024

Citation: Finelli, R.; Sena, P.; Lorusso, A.; Cecere, L.; Villecco, F. Reproduction of Road Scenarios for Simulated Driving Using LiDar Surveying Technique. *Machines* **2025**, *13*, 4. https://doi.org/10.3390/machines13010004

Copyright: © 2024 by the authors. Licensee MDPI, Basel, Switzerland. This article is an open access article distributed under the terms and conditions of the Creative Commons Attribution (CC BY) license (https://creativecommons.org/licenses/by/4.0/).

1. Introduction

Over the years, thanks to technological progress, the study of simulation and, consequently, three-dimensional modeling has become increasingly present and active in various fields of research. In particular, driving simulators are useful aids in industry and beyond: from the design of road vehicles [1], intended for the public market, to the analysis of the driving performance of Formula 1 drivers [2]. Simulators are therefore used for driver training, engineering research, and vehicle development, as well as in the ergonomic and psychological analysis of driver driving behavior. Engineers use driving simulators to study driver–vehicle interactions, aiming to develop optimal solutions for car design. These devices present an advantageous alternative when compared to traditional test rides performed on road [3]. For this reason, research in this regard is in continuous development.

The main points in favor of driving simulation include increased safety, complete control of experimental conditions, reduced cost and time, and reduced environmental impact. The most evident advantage is the total absence of danger, even in situations that on a road would pose a risk to the driver. This allows for the simulation of emergency

situations and driver training without real physical consequences [4]. Complete control of experimental conditions is particularly evident in the world of motorsport (for example, in Formula 1, where environmental conditions can significantly influence the fate of a race). Through a driving simulator, various race factors, such as time of day, weather, and, consequently, asphalt temperature, can be set. The various driving conditions can then be changed at any time, providing a wide versatility of settings [5].

Testing a car before a competition or market launch is a crucial part of the vehicle development process, involving significant costs and time to fully validate the proposed model. A simulator, on the other hand, allows test rides without the costs of vehicle maintenance, track management, and fuel consumption [6].

Additionally, a driving simulator is also a green alternative capable of reducing CO_2 emissions from road test rides [7].

These advantages have fueled the driving simulator's rapid evolution across various application fields. In addition, it is important to note that driving simulation is one of the most studied areas of virtual reality, and not only in research fields, as it has garnered significant interest from the gaming community, representing one of the most popular game categories.

For this very reason, the simulator is a complex system equipped with hardware and software, each with its own role, capable of recreating realistic and immersive driving [8].

Realism is therefore a prerequisite for the proper use of a driving simulator [9], whether this is for recreational [10] or research purposes [5]. Without it, test rides would not be comparable to tests performed on the road and, consequently, would be invalid for the purposes of experimentation. Therefore, there is great interest and continuous development in narrowing the gap between the real world and the virtual reality in the laboratory. By analyzing the components of which the simulator is composed [11], it is possible to group them into several basic categories.

The hardware components comprise the cockpit, which includes a driver's seat; a realistic steering wheel with force feedback for enhanced driving feel; a set of pedals with accelerator, brake, and clutch; and, finally, a potential physical dashboard. However, this dashboard is not always physically present but rather appears in a virtual version within the selected car's view. For a more complete driving experience, an advanced display system is essential. A VR visor or a set of three panoramic screens can comprise this system, enhancing the realism of the experience. By simulating every sound associated with the car and its surroundings, the sensory system enhances the audiovisual sensory experience. As shown in Figure 1, driving simulators usually come in two different layouts: fixed-platform and motion-based driving simulators [12,13].



(**a**) (**b**)

Figure 1. (**a**) Fixed-base driving simulator—texgroupitalia.com; (**b**) Motion-based driving simulator—www.motorvalley.it, accessed on 1 September 2024.

Specifically, the fixed-platform [14–16] (fixed-base driving simulator) consists of a structure welded to the floor (Figure 1a); as a result, audiovisual reproduction is responsible for simulating all driving effects.

On the other hand, the motion-based driving simulator features a mobile platform [2,17,18] (motion-based driving simulator), where the driver's station is connected to the floor via a hydraulic press system capable of reproducing most of the vehicle's movements (Figure 1b).

In conclusion, the motion-based simulator provides a significantly more advanced driving realism compared to a fixed-platform simulator [19]. This is achieved by replicating the vehicle's accelerations, braking forces, and lateral forces, such as centrifugal forces during cornering, as well as the driving trajectory of the vehicle. Continuing with the software components, it is clear that in order to provide advanced virtual-reality driving, simulation software with a graphics engine capable of faithfully reproducing images of the track, the surrounding landscape, and any other vehicles on the track is essential.

So far, the use of laser scanners has been mainly focused in other fields of engineering [20–22] and architectural applications, while in the automotive sector they have been mainly used for the design of autonomous vehicles [23,24]. However, their use as a means of acquiring real automotive tracks is still a developing and expanding field.

The goal of this study was to replicate a real road scenario for importation into driving software.

To create the virtual scenario in question, it was necessary to edit and import a real track present within the Fisciano campus of the University of Salerno into Assetto Corsa driving software.

The paper is structured into six sections aimed at providing a thorough description of the workflow.

Specifically, Section 2 introduces the fields of driving simulation, 3D modeling, and, in particular, track design. Furthermore, it showcases the existing approaches to designing a driving track, which are not the same as the one this paper adopts.

Subsequently, Section 3 delineates the necessary procedures for data collection and processing, which are essential for modeling the selected real track for the case study.

Section 4 describes the survey and analysis conducted within the Fisciano campus of the University of Salerno.

Finally, Section 5 reports the results of the work carried out, leading to the conclusions presented in Section 6. This final section deduces conclusions from the completed work and suggests potential future advancements to improve the previously presented work.

2. State of the Art

This section outlines the development of driving simulators and the techniques used to date for track acquisition and modeling.

The driving simulator began its spread in the first decades of the 20th century [12]. At that time, the use of these devices was limited to driver training; later, it spread to the automotive industry to test new vehicles by crash testing and to test new ergonomic solutions. Over time, research institutes and technical universities have become increasingly interested in simulators. The interest stems from several strategic factors, such as the ability to set up, check, and repeat various driving configurations in complete safety while reducing the expected costs of any real on-road tests. The simulator is also used in the medical field [12], in which the driving ability of patients suffering from impaired performance due to a variety of medical causes is analyzed. The applications of the driving simulator may also belong to a purely psychological field of interest [25]. Moreover, as noted in the previous section, driving simulators are sustainable and environmentally friendly.

Another great utility of simulators is related to the world of motorsport; racing teams can, in fact, find great support from driving simulation. Specifically, in the realm of Formula 1, the simulators utilized by various teams represent the most advanced software available on the market. In fact, these devices provide a wealth of information about the driver's performance during a single test ride. Also, in the world of motorsport, another advantage, already analyzed in the previous section, is certainly the absolute safety compared to on-road tests that subject drivers to high-risk situations. In addition, on the track, the total cost budget is also greater [12,26] (in each test ride, the driver consumes a minimum of one to two sets of tires, and if the car suffers damage, the team has to repair or change the broken components before the race).

In high-level sports competitions, the reliability of testing is fundamental to vehicle design and mapping. Therefore, it is vital to pay attention to the design of driving tracks [27]. Each championship circuit has its own characteristics, and training drivers for each circuit before a race is a key element for the successful performance of the drivers. Naturally, the more detailed the virtual model of the track is, the more accurate the test ride results will be compared to reality, and thus there will be fewer errors during the race. For this reason, the various studies carried out with different data collection methods available on the market will be proposed and compared based on various parameters to determine the most convenient available methodology.

These days, most driving simulators model their tracks using data from real circuits. For this reason, there are various methods for obtaining the coordinates of a track. It is understood that the degree of definition of the collected data varies depending on the hardware used. The different track design methods also differ in terms of the designer's economic accessibility, the availability of products on the market, and the complexity of data acquisition and processing.

The simplest way to acquire the data is through digital maps already available online (2D models). Another approach could be using a laser scanner (3D models). The disadvantage of using digital maps lies in the coordinates of the acquired points. Digital maps only offer the X and Y coordinates of each captured vertex. For this reason, other methodologies typically complement digital map acquisition by providing the Z coordinates. For instance, to obtain a valid 3D model, devices like drones, GoPro cameras [28], and the Zed Mini Stereo Camera might be necessary [29]. On the other hand, the laser scanner is as effective as it is complex. The device takes a 360° photo and superimposes it onto an infrared light beam-derived point cloud of the surrounding environment. All these devices are capable of capturing photos or frames that contain the necessary information for generating a new point cloud through photogrammetry.

Photogrammetry is a method of reconstructing 3D models using photography [22,30–32]. It is used in various fields such as geomatics [33], topography [34], architecture [35,36], archeology [37,38], and other engineering fields [39]. The high costs of the necessary equipment limited the possibility of using this technique until a few years ago. However, thanks to advancements in computational graphics and the availability of increasingly powerful computers, this technique has become simpler and more affordable to manage [40], but also more reliable, economical, and precise for obtaining topographic data [41].

This process, considering one kilometer of track, takes about two working weeks of design and a medium–low project budget, which includes the purchase of a camera, a drone, and necessary editing software. While the project results may not be as precise as they could be today, the speed and versatility of data acquisition continue to be an advantage.

Below is a summary (Table 1) of the various three-dimensional point acquisition methods for a track, highlighting the advantages and disadvantages to consider during the design phase.

Table 1. Different types of method useful for modeling a racetrack.

Methods	Advantages	Disadvantages
Digital Maps	Quick, economically accessible, readily available	It only provides X and Y coordinates, insufficient for full modeling of a 3D track
Laser Scanner	Highly accurate, detailed point clouds	Complex, expensive, it requires advanced equipment
2D Models	Fast data collection, suitable for simple simulations	Limited to lateral movement, lacks depth (Z coordinates)
3D Models	Complete, quick transition from reality to virtual reality	It requires specific devices (drones, cameras)
Photogrammetry	Reliable, cost-effective, precise	Long editing process, it requires powerful computers

After careful analysis of the state of the art, a measurement technique involving the use of a laser scanner was chosen to acquire the geometric territorial information of the track examined in the case study.

3. Materials and Methods

This work aims to propose an innovative methodology for data acquisition and processing to be imported into the driving simulator's scenario. This procedure considers a point acquisition device, such as a laser scanner, capable of obtaining both graphical information useful for texture mapping and three-dimensional points. A laser scanner is an indirect survey technology that allows for the accurate acquisition of most of the information regarding the topographic features of a track [42]. Following an initial data acquisition phase, to enhance the obtained scans, a post-processing phase follows in which the scans are modified and cleaned of any graphic or geometric errors.

Since this technology represents an innovation in the field of automotive track design, it is necessary to understand its positive and negative aspects that differentiate it from other data collection devices. The measurement technique used is called LiDAR (Laser Imaging Detection and Ranging) [43,44]. Thanks to this technique, objects along the laser's path reflect the light beam back to an internal sensor in the scanner [45,46]. This allows the device to capture millions of three-dimensional points, known as PCD (point cloud data). The point cloud can subsequently be interpreted as a three-dimensional geometric model.

The following Figure 2 introduces the main phases that led to the reproduction of the real track in the virtual world of the simulator, which will be described in more detail in the case study.

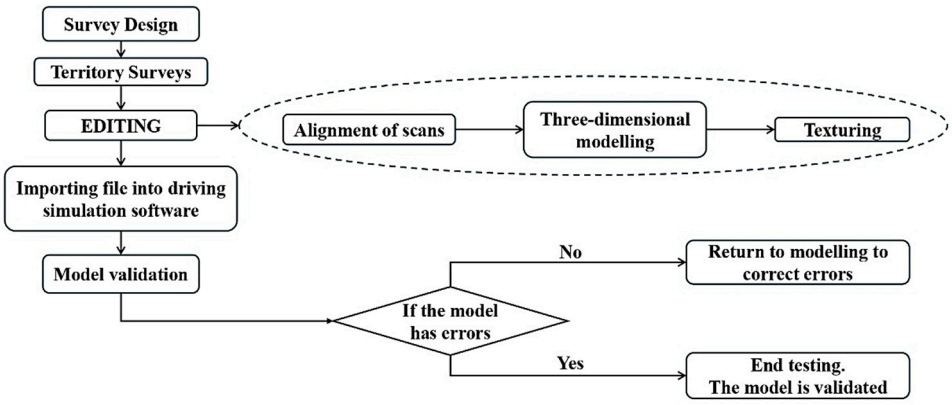


Figure 2. Graph approach workflow.

First and foremost, understanding the information from the track is crucial. Based on this, the survey phase needs to be structured accordingly. The track is then scanned using a laser scanner. Depending on the length of the track, this step could take several days due to potential issues related to weather, temperature during the surveys, and other factors that could affect the proper functioning of the laser scanner. After completing the surveys of the entire circuit, a post-production phase follows, in which the various scans are imported into the modeling software. First, the scans are aligned, then cleaned, and, finally, each object in the point cloud is assigned a specific texture and material. These steps are essential for the proper functioning of the track, as the simulator must be able to recognize each object within the three-dimensional model.

Once the final project is corrected and perfected, it is time to export it from the modeling program to the driving simulator. It is essential that the track model format for this step is FBX (Filmbox) [47,48]. This proprietary file format (.fbx) was developed by Kaydara and has been owned by Autodesk since 2006. It is used to ensure interconnectivity between various programs designed for creating digital content [49]. This type of file is associated with PNG (Portable Network Graphics) or DDS (DirectDraw Surface) files containing the textures needed to color the polygonal mesh [50]. After importing the project into the driving software libraries, it is time to test its validity and realism. This involves a series of test rides aimed at the final validation of the model. Tests are conducted first to ensure the correct reading of the imported folder in the program and to test the correct movement of the vehicle within the track.

If the model does not pass the tests, showing discrepancies with the real track or presenting reading errors caused by the driving software, an iterative process continues until the model functions correctly. For instance, if the track contains missing points, the process reverts to the post-production phase to reconstruct the damaged track model. If a new scan is needed, the survey phase must be repeated along with all subsequent steps to avoid the original problem.

The model validation takes place in the simulator, whose overall structure it is important to define. The simulator can be described as a set of blocks, each managing a specific aspect that characterizes the driving performance [11,51]: the driver, vehicle model dynamics, control systems, audiovisual devices, and the virtual environment. First of all, the driver receives stimuli from the software's audiovisual interface (and the movements of the motion platform) and responds to them by interacting with the track through the associated vehicle model.

Then, the vehicle model dynamic block responds to driving physics, replicating the vehicle's movements on the track. It is created with various items of information dependent on the driver's actions on the track.

Control systems, such as the steering wheel, brake, accelerator, clutch pedals, and gearbox, allow the driver to maneuver the vehicle.

Audio and video devices, including screens and speaker systems, are designed to enhance the driver's driving experience. The virtual environment, which is the primary focus of this study, forms the visual system's core element, featuring the driving track with which the driver interacts [52].

In the case study, a simulation system with a mobile platform will be examined. This system is further complicated by three additional subsystems: the platform drive logic, a platform kinematic model, and a platform trajectory. The platform drive logic refers to the control and management system that coordinates the movements of the dynamic platform on which the simulator is mounted. The platform kinematic model establishes the degrees of freedom of the platform and processes kinematic equations to determine the structure's movements, providing the mathematical basis for the platform drive logic.

While the drive logic controls the actuators in real time, the kinematic model ensures that the commands sent to the actuators produce the correct movements. Finally, the platform trajectory calculates the ideal path the platform should follow to replicate the vehicle's movements, providing the platform with the necessary information to connect the movements of the station with the driving interface [53].

4. Case Study

In this section, the workflow necessary for the creation of the circuit in virtual reality is analyzed.

The chosen circuit is circa 1001.90 m long and covers an area of 25,641.90 square meters. It has a maximum slope of 16.1% and −19.1%, with an average slope of ±4.5%. The altitude ranges from 266 m to 276 m, with an average of 271 m. Therefore, the surveyed surfaces are paved roads, along the edges of which there are almost always sidewalks made of bricks and hedges or lawns.

The laser scanner used for completing the case study was the Leica BLK360 (Leica BLK360 producted and distribuited by Leica Geosystems AG–Part of Hexagon, Heinrich-Wild-Strasse, 9435 Heerbrugg, Switzerland). The use of this new technology allowed the obtainment of both panoramic images of the surrounding environment, thanks to the HDR camera, and complex point clouds due to the infrared light beam emitted by the scanner. Delving into more detail, the various stages of the work carried out can be elaborated as follows: terrain analysis and survey planning; field survey; exporting and correcting the scans, from point cloud to mesh; and model validation.

The study began with an investigation of the terrain aimed at understanding the optimal path for data acquisition and identifying any potential complications. For the case study under consideration, a closed route within the Fisciano campus of the University of Salerno was chosen to best simulate a car racing track. The route includes the streets Via Francesco De Sanctis, Via del Diritto, and Via della Tecnica. The project involved a scan every 10 m, more than recommended in the Leica BLK360 user manual [54], to avoid significant difficulties in overlapping scans. This is because the scans, in order to be correctly aligned, must contain a certain percentage of common points; otherwise, the entire point cloud would not be robust enough.

Given the length of the circuit and the decision to perform one scan every 10 m to densify the point cloud, a total of 100 scans were conducted (Figure 3). Of these, 12 scans were repeated due to the presence of noise caused by the movement of unwanted subjects, such as people and vehicles, during the scanning process.



Figure 3. Racetrack shown with all the scan points (blue pins) and the start point (yellow pin)—earth.google.com, accessed on 10 April 2024.

The path having been chosen, the next step was starting the survey with the laser scanner. The Leica BLK360 generates high-precision point clouds [54]. The scanning system is a high-speed ToF unit, enhanced by Waveform Digitizing (WFD) technology; the maximum scanning frequency is 360,000 points per second [54]. The device is capable of capturing points at a minimum distance of 0.6 m up to a maximum of 60 m. This technique determines the distance from an object or surface using a laser pulse. The laser scanner emits an infrared light beam that reflects off a rotating prism, which colors the surroundings of the device. The prism then rotates, moving the laser over the object or surface [44,55].

The field of view features a 360° scan (horizontal direction) and a 300° scan (vertical direction). The device is equipped with three 15 Mpixel cameras with a maximum resolution of 150 Mpx, HDR, and an LED Flash, ensuring clear images even in darker environments. Additionally, the laser scanner used has a FLIR longwave thermographic camera [56] with 360° × 70° (horizontal × vertical) coverage. The route selection also took into account the flow of people and vehicles in the selected part of the campus. This is because the device needs to remain in the survey position for about three minutes, of which 1 min and 50 s (Table 2) are needed to obtain the point cloud, while the remaining seconds are necessary for acquiring the thermal image and the panoramic image.

Table 2. Scan duration for three settings and image capturing time—Leica BLK360 User Manual.

Point Density Mode	**Resolution [mm @ 10 m]**	**Estimated Scan Duration [MM:SS] for a Full-Dome Scan**
Fast	35	00:40
Standard	10	01:50
High-density	5	03:40
Camera Type	**Estimated Image Duration [MM:SS]**	
Non-HDR	01:00	
HDR	02:30	
Thermal	00:30	

The acquisition mode chosen during the field surveys was the standard one, corresponding to a three-dimensional point resolution of 10 mm at 10 m. Another factor to consider during the scans was the weather forecast.

Rainy or windy conditions could interfere with data reception, contaminate the cameras and sensors, or even damage the Leica BLK360.

During the survey, weather conditions presented a challenge, as the data collection was carried out over three days in April, with temperatures reaching approximately 27–28 °C under clear skies. Due to solar radiation and the high perceived temperature, the workflow experienced delays, as pauses were required, and some scans needed to be repeated. This was necessitated by the operational limitation of the Leica BLK360, which cannot function at temperatures exceeding 40 °C [54].

Another factor to consider was the presence of shadows along the route. Since the survey was conducted over three days, from morning to afternoon, certain sections of the road exhibited shadows at varying angles. A potential solution to this issue could have been to perform the scans within the same time frame each day but on different days, ideally under slightly overcast conditions to minimize the impact of direct sunlight and shadow variability.

In conclusion, a total of 112 scans were actually obtained due to some issues caused by unfavorable conditions, particularly near the canteen where the flow of people was consistently high throughout the day. In total, considering approximately 3 min per scan

multiplied by the 112 scans performed over three days of acquisitions starting around 10:00 a.m. and ending around 7:00 p.m. with a 2 h and 30 min break, about 19 h and 30 min of gross work were spent, of which 5 h and 36 min were dedicated to the scans alone.

$$N_{total\ gross\ h} = [(19 - 10)\ \text{h} - 2.5\ \text{h}] \times 3\ \text{days} = 19\ \text{h}\ 30\ \text{min} \quad (1)$$

$$N_{total\ net\ h} = \frac{112\ \text{scans} \times 3\ \text{min}}{60} = \frac{336}{60} = 5\ \text{h}\ 36\ \text{min} \quad (2)$$

Following the acquisition work, the process continued with a post-production phase where the scans were modified, cleaned, and optimized for the driving software Assetto Corsa v1.16.

Before starting the editing process of the scans, it was necessary to use the BLK Data Manager 2023.1.0 software to transfer all the scans acquired from the internal memory of the Leica BLK360 (the device can store up to 100 scans) to the working computer. The scans are imported to the computer in .blk format, readable only by Leica proprietary software. For this reason, the work continued with the Leica Cyclone Register 360 Plus v2023.1.0 software, used for aligning and cleaning the scans.

Cyclone offers three viewing modes [57]: "SiteMap", "Bundle Cloud", and "TruSlicer". The SiteMap visualization provides an overhead view of the entire site (Figure 4). Activating the commands in the software's graphical interface enables the display of blue points representing the performed scans. Each point is connected to its neighbors by a line that represents the alignment between the two scans under consideration.



Figure 4. Leica Cyclone Register Plus 360—SiteMap.

The second viewing mode, the "Bundle Cloud", allows for a three-dimensional view of the entire site and is particularly useful for isolating individual scans for modification and cleaning (Figure 5). In this mode, it is possible to verify the robustness of all alignments; if an alignment is not sufficiently robust, the line associated with the compromised alignment will appear yellow or red, depending on the severity of the overlap error between the two scans.

Finally, the last mode, "TruSlicer", enables color-coded scan identification to facilitate differentiation (Figure 6). This feature is particularly helpful during scan cleaning. For instance, if an object captured during one scan is adjacent to another scan in which the

moving object is no longer present, it is possible to distinguish which scan needs to be cleaned without altering the clean scan.

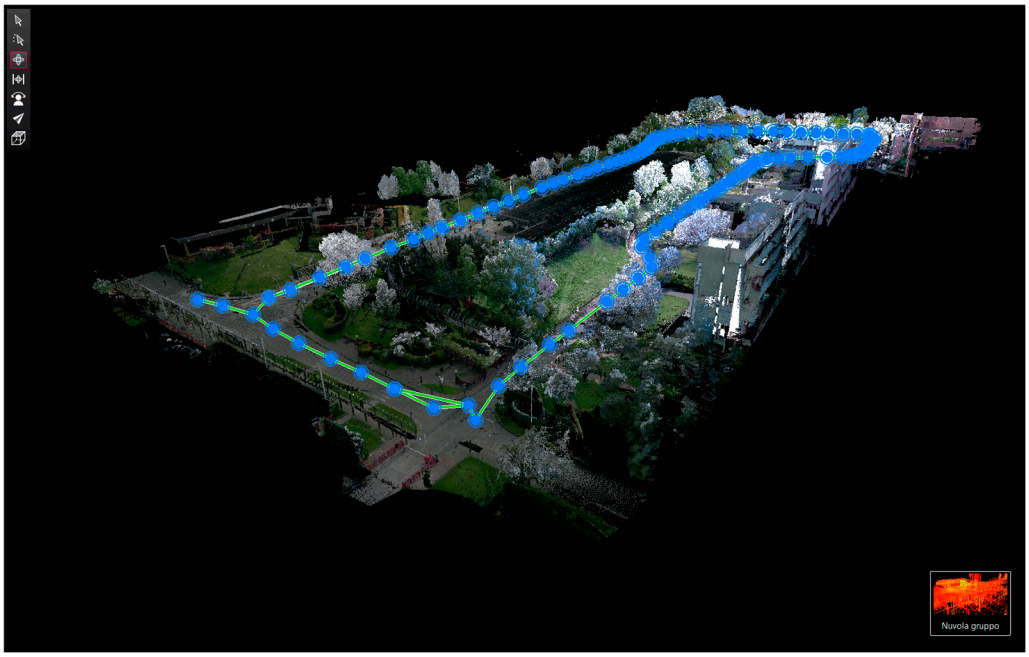


Figure 5. Leica Cyclone Register Plus 360—Bundle Cloud.

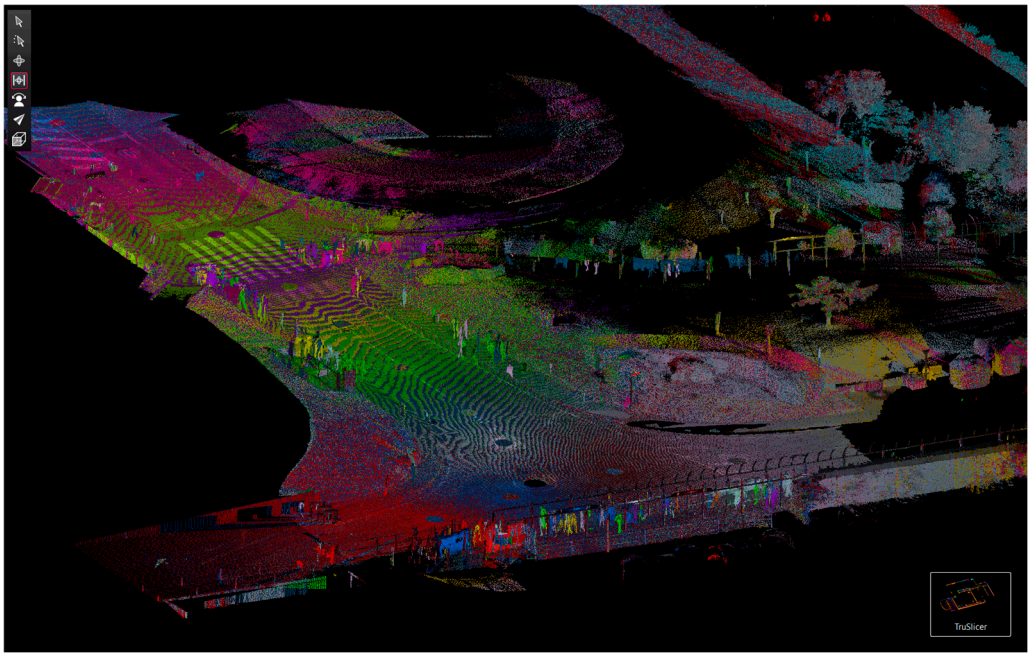


Figure 6. Leica Cyclone Register Plus 360—TruSlicer.

The software allows for the alignment (this step may take from a few minutes to several hours, depending on the number of scans to be processed) and cleaning of potential disturbances from the various scans, such as people or vehicles present at the time of scanning. The main objective was to make the road and sidewalk passable for the car in Assetto Corsa. In Cyclone software, the alignment between two adjacent scans can be performed through [57] a visual alignment (Figure 7) or a point alignment with dual visualization (Figure 8). The visual alignment feature allows overlapping of common points between two scans, identifiable by two different colors, blue and orange. Alignment can be performed from both a side view and a top view, and it is possible to translate and rotate

one scan relative to the other to achieve the highest precision in the overlap. Additionally, in this mode, it is possible to remove any disturbing elements that reduce the robustness of the alignment, such as trees and hedges along the roadside. Thanks to its ease and speed of use, visual alignment was the most utilized method in this case study.

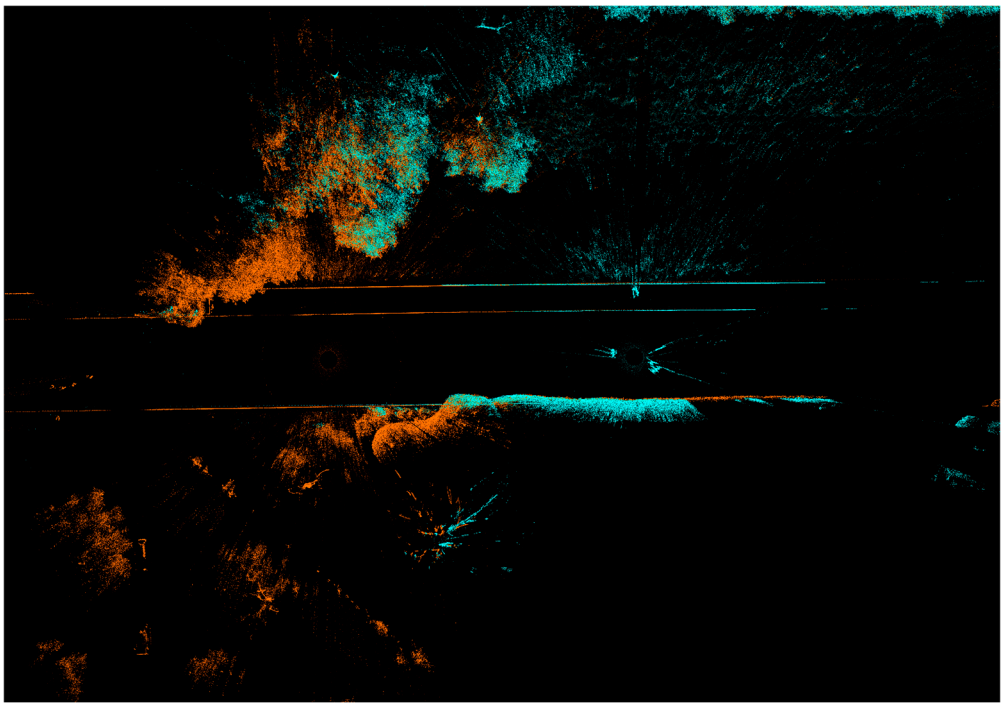


Figure 7. Leica Cyclone Register Plus 360—Visual Alignment.

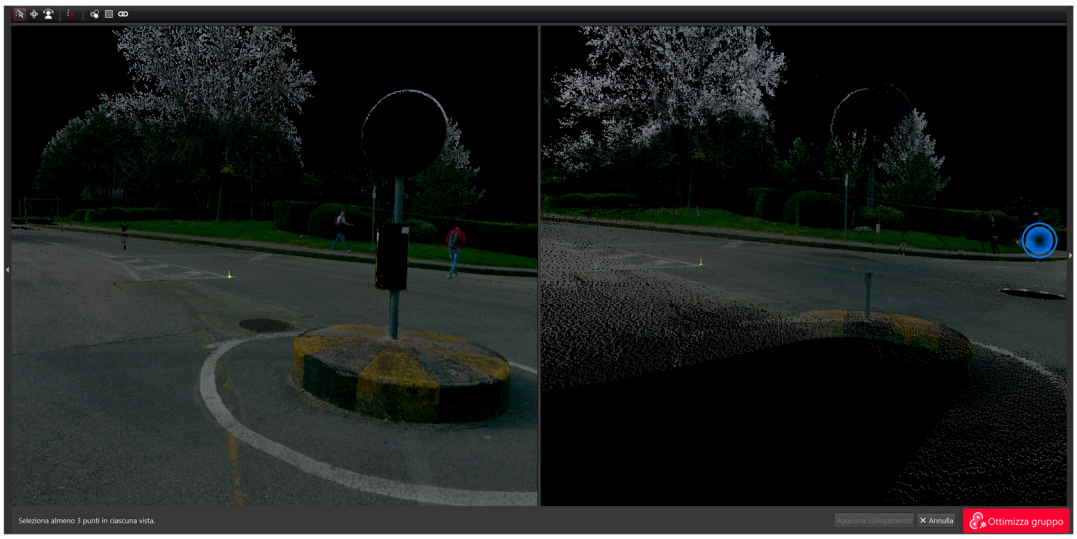
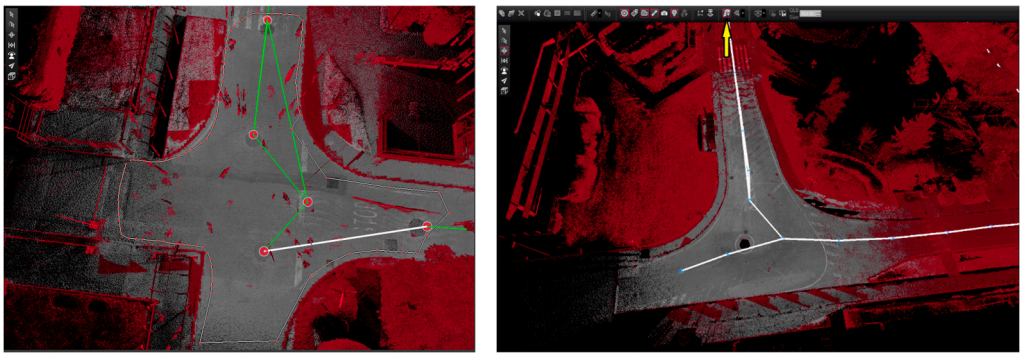


Figure 8. Leica Cyclone Register Plus 360—a point alignment with dual visualization.

On the other hand, point alignment with dual visualization (Figure 8) involves identifying three common points between two scans. This type of alignment would have been more effective than the first if targets had been used during the scanning process to facilitate the recognition of the three points between the scans. Unlike the first method, this second type of alignment does not allow for scan cleaning, which slows down the construction process of the entire circuit.

Switching to the "Bundle Cloud" view mode and using the "Detect Smooth Surface" function enabled the elimination of floating points above smooth surfaces, such as roads

and sidewalks (Figure 9). This command is particularly useful, as it removes all disturbance points on flat surfaces, leaving them intact and clean. However, the process required several days to complete. While the software efficiently processes commands, the cleaning procedure demands exceptional precision and attention to detail to avoid deleting essential points.



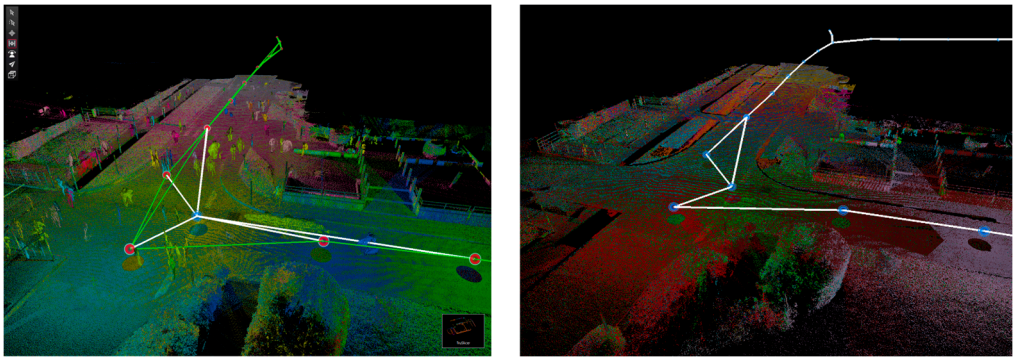
(**a**) (**b**)

Figure 9. (**a**) Smooth surface (uncleaned road), with green lines representing the links between the scans and a single white line representing the selected link—Leica Cyclone Register 360 Plus; (**b**) smooth surface (cleaned road), with a yellow arrow which points to the smooth surface button—Leica Cyclone Register 360 Plus.

A specific challenge arose from the function's reliance on identifying flat surfaces. For example, when points were located above the elevation difference between the sidewalk and the road, the software failed to recognize the step as part of a continuous flat surface. This issue led to the unintended removal of points at the interface between the sidewalk and the road. Figure 9a illustrates this problem, showing a band of red points following the sidewalk's profile.

To resolve this issue, it was necessary to carefully adjust the viewing angle during the selection of points for removal. This step required significant attention to ensure continuity between the road and the sidewalk. This precision was critical, especially since the vehicle had to be able to transition smoothly between the road and the sidewalk without its wheels encountering gaps at the sidewalk step.

Once all the scans of the circuit were aligned, using the "TruSlicer" view mode, it was possible to identify the last points to be removed (Figure 10).



(**a**) (**b**)

Figure 10. (**a**) Leica Cyclone Register Plus 360—not-clean point cloud; (**b**) Leica Cyclone Register Plus 360—clean point cloud.

Before continuing with point cloud editing, it was advisable to create a folder to store all the information related to the track. This folder had then to be imported directly into the Assetto Corsa libraries. It was essential to use the correct nomenclature and file format.

The files required for encoding the track were stored in specific subfolders.

The "ai" subfolder contained the information necessary for the AI (Artificial Intelligence) to recognize and use the track.

The "data" subfolder included parameters related to surfaces, cameras, and audio sources within the simulation, which can be defined and modified.

Among these, the most critical file for track configuration is "surfaces.ini" (Figure 11). For this case study, only this file was modified, as the other files contained information about the layout and virtual driving scene, which were largely standardized and therefore did not require customization for each newly created track.

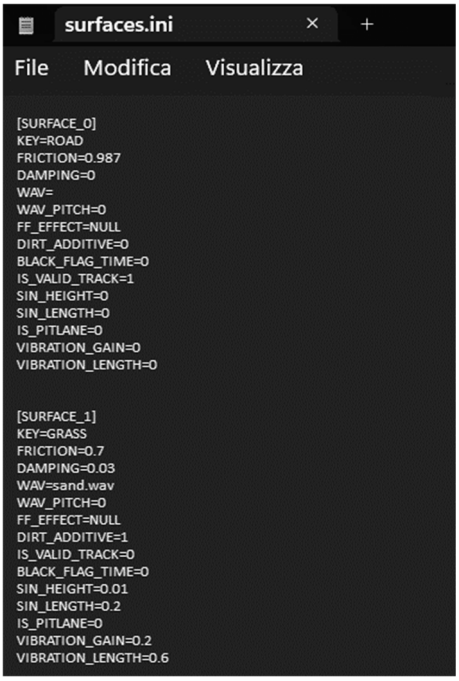


Figure 11. File surface.ini.

As shown in the Figure 11, the file structure allows the definition of a specific surface type, such as the "road", and the adjustment of all relevant parameters.

For this study, the "FRICTION" parameter, which defines the surface's coefficient of friction, was set to 0.987. A higher value corresponds to a greater tire grip on the surface. The "DAMPING" parameter, which governs the damping effect on motion, was set to 0. If activated, this parameter can affect the surface's ability to absorb energy, such as impacts or oscillations.

The "WAV" and "WAV_PITCH" parameters refer to the path of an audio file associated with the surface. In this case, they were not enabled.

The "FF_EFFECT" parameter specifies the force feedback effect applied to the steering wheel when interacting with the surface, if present.

The "DIRT_ADDITIVE" parameter allows for the accumulation of dirt on the tires, influencing their performance.

The "BLACK_FLAG_TIME" parameter enables the assignment of a penalty if the driver remains on this surface for an extended period.

The "IS_VALID_TRACK" parameter determines whether the surface is part of the valid racing track (a value of 1 validates the surface).

The "SIN_HEIGHT" and "SIN_LENGTH" parameters specify the height and wavelength of sinusoidal undulations on the surface, respectively, enabling the creation of irregular surfaces.

The "IS_PITLANE" parameter indicates whether the surface is part of the pit lane.

Finally, the "VIBRATION_GAIN" and "VIBRATION_LENGTH" parameters define the intensity and duration of vibrations experienced when the vehicle traverses a surface. Particular attention should be paid to these two parameters; for example, in the case of the "GRASS" surface, these values were set to 0.2 and 0.6, respectively.

By carefully configuring all necessary parameters, it was possible to optimize the driving experience, differentiating the sensations and associated movements that the driver perceives during the test-ride phase.

The "ui" subfolder is where the basic track information is recorded: the outline, which is a summary image of the track profile; the preview, which is the presentation image of the track; and the ui_track.json, which contains additional information useful for displaying the track in the main menu. These three files allow the software to insert the track into the initial track selection screen. Then, there is also a "map.png" image used by the program as the track image and a "unisa_track.kn5" file, which contains all the information related to the geometry, materials, and textures of the track.

After creating the Assetto Corsa folder, the primary file derived from processing the point cloud was in KN5 format. This format is usually associated with Kunos Simulations software, such as Assetto Corsa. Conventionally, these files are considered formatted as Assetto Corsa 3D Objects and appear mainly in the Game Files section. To obtain a file in .kn5 format, the point cloud is imported and exported through various 3D modeling software packages, transforming the point cloud obtained from real track scans into a polygonal mesh of the simulated track model.

In computational graphics, a polygonal mesh is a grid defining an object in space, composed of vertices, edges, and faces. More specifically, a mesh (literally, "net" or "grid") is the subdivision of a continuous surface into polygonal cells, such as triangles, quadrilaterals, etc.

This format transition is necessary because, unlike the mesh, the point cloud cannot be recognized by the AC (Assetto Corsa) driving program as a physical object on which the car must move. Therefore, the point cloud is first exported from Leica Cyclone Register Plus 360 in E57 format along with the panoramic images of each scan. Then, the file is imported into Metashape, where it is possible to transform the point cloud into a mesh using the Workflow > Build Mesh command [58] (Figure 12). This is performed in sections to speed up the process. This process was carried out by dividing the circuit into sections, as the point cloud contained too many points to be processed without subdivision into smaller areas. As shown in Figure 12, the peripheral areas surrounding the road, located at a significant distance from the laser scanner, exhibit a lower point density. Consequently, the final result of the mesh construction revealed gaps in these areas.

This, however, did not pose a problem, as a lower point density had been intentionally planned for gardens and other areas where the vehicle was not expected to pass. This approach ensured a denser mesh along the road and sidewalks, while simplifying the peripheral zones, ultimately reducing the size of the final file.

Once the 3D model of each part is obtained, it is exported in FBX format, ready to be imported into Blender.

The mesh must now be modeled and reconstructed with all the parameters required by Assetto Corsa [45]. At this point, the nomenclature from the surfaces.ini file in the track folder is followed. The road, grass, buildings, and trees must all have associated and distinct names (Figure 13), materials, and textures.

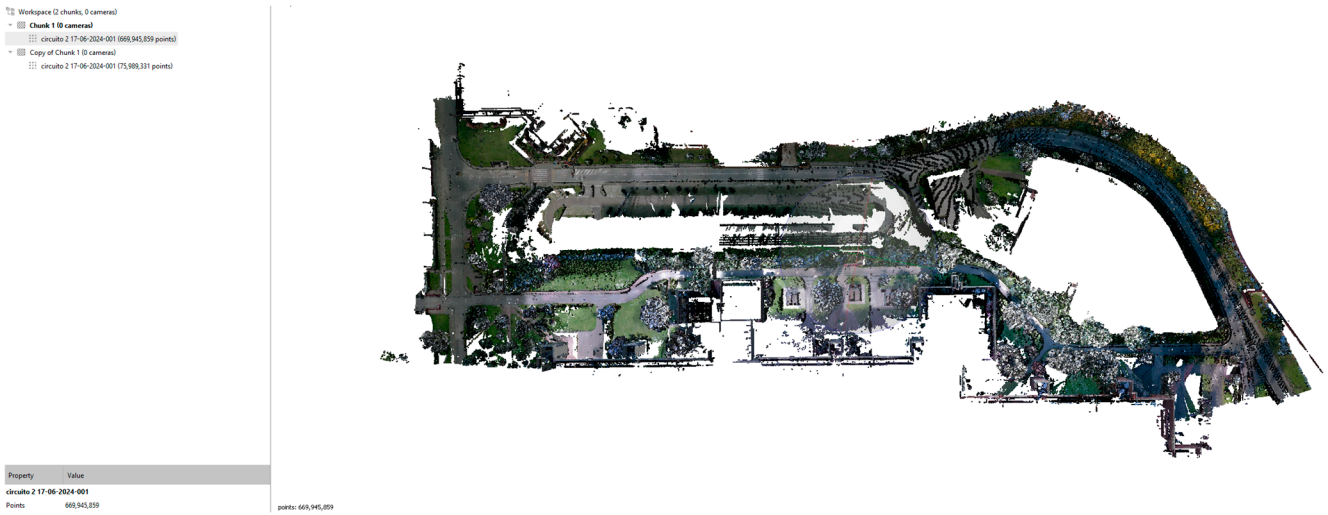


Figure 12. View of the point cloud in E57 format—Agisoft Metashape.

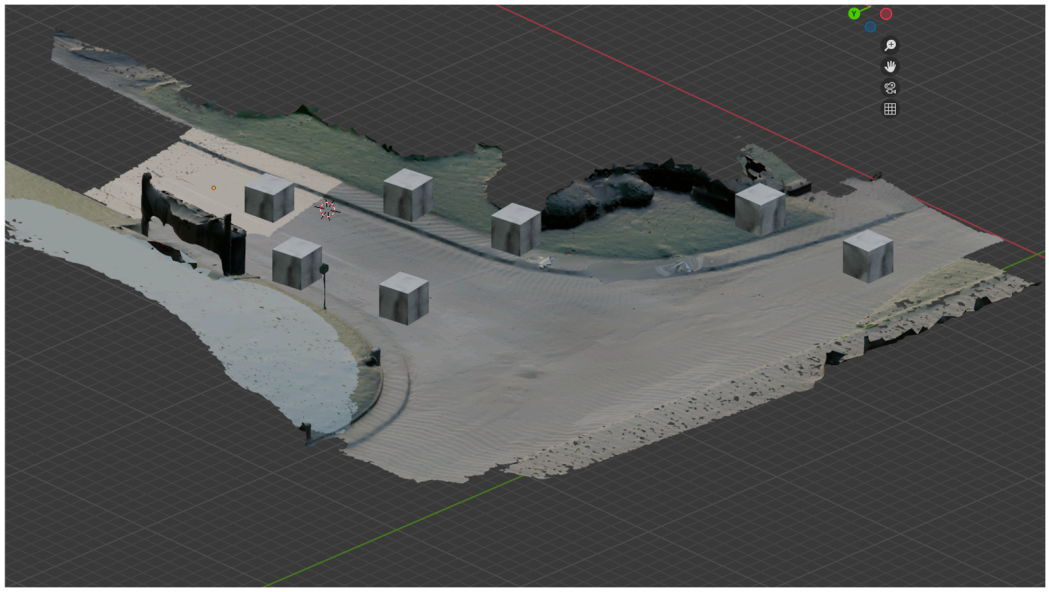


Figure 13. RGB-colored mesh in Blender.

The road is saved in Blender's Outliner as a physical object named "1ROAD". This allows the car to move on the selected mesh part without the risk of falling into the void, which is precisely what we want to avoid when modeling a track.

The grass (1GRASS) bordering the road will have different characteristics compared to 1ROAD. Indeed, the vibration and friction data (FRICTION) in the surfaces.ini file related to the grass differ from the data for the road. This naturally increases the realism and validity of the track being modeled [59].

It is mandatory to insert a collision element in the mesh. While roads, grass, etc., are physical objects on which the car must move, the WALL is a simple collision mesh identifying the selected mesh as an obstacle for the car. This prevents the car from falling into the void, circumscribing its movement area.

Regardless of the complexity of the track being modeled, spawn objects are essential for the track to function in all driving modes (races, hot laps, and practice).

Therefore, cubes are added to the track and named according to Assetto Corsa's nomenclature: AC_START_0 and AC_START_1, identifying the start line where the car is positioned at the beginning of a lap; AC_PIT_0 and AC_PIT_1, identifying the pit area; AC_HOTLAP_START_0, marking the beginning of the timed lap; AC_TIME_0_L

and AC_TIME_0_R, where the program marks the start lap time; AC_TIME_1_L and AC_TIME_1_R, where the program calculates intermediate times.

At this stage, the texture and material of each object define all of its physical characteristics.

Furthermore, the texture creation process in this case study presented several challenges, as various procedures were tested to achieve an RGB-colored mesh. Among the various texture creation methodologies, the software Meshlab was utilized. The advantage of Meshlab is that, from a colored point cloud, a file containing the texture (mesh_1.png) can be derived, along with a file (mesh_1.obj) containing only the mesh, which is importable into Blender. However, a problem arose when the software attempted to process a point cloud that was too large and complex. Attempts to simplify and divide the cloud into sections proved futile and inefficient for the simplification process.

Another approach considered was the use of digital drawing programs such as GIMP and Materialize. These programs, primarily used for creating textures from point clouds obtained through photogrammetry, require orthophotos, which contain different information from the panoramic images taken by the Leica BLK 360.

Finally, a texture file in .png format was created using Metashape 2.1.4. In Figure 14, the result of this process is shown. After creating the polygonal mesh in Metashape, a PNG texture file can be obtained by selecting Workflow > Build texture.

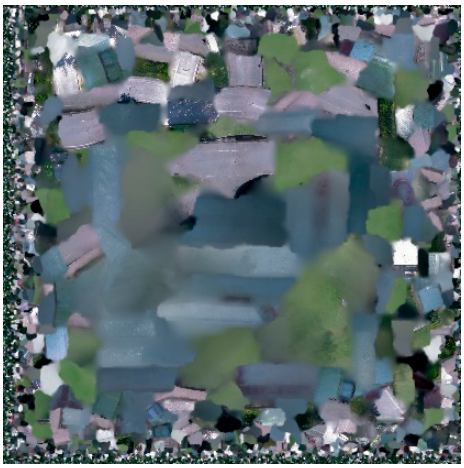


Figure 14. Diffuse texture of a section of the Unisa racetrack—Agisoft Metashape.

The colored faces of the mesh were selected as the texture source, with a resolution of 4096×1 to ensure high graphic definition without it being too cumbersome to manage. The texture was then associated with the mesh in Blender.

The editing and transformation phase of the point cloud into the mesh took approximately three weeks of work. The time required is closely dependent on the length of the chosen track and the number of disruptive elements present in the various scans.

Once the file was obtained in .fbx format along with the folder containing all associated textures, the software KSEditor v6 (Figure 15) was used to verify all characteristics of the track model and set the climate, shaders, visualization, and shadows on the track. The track was then exported from KSEditor in .kn5 format, containing both texture information and mesh geometry. The folder was subsequently placed in the Assetto Corsa libraries via the path [Steamapps > common > assettocorsa > content > tracks].

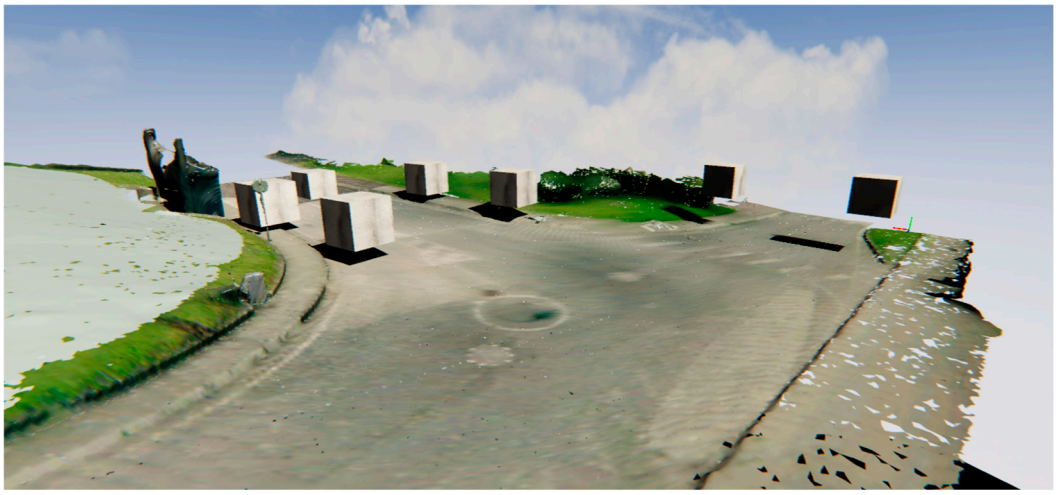


Figure 15. A section of the Unisa racetrack imported in KSEditor.

Finally, the track needed to be tested with test rides during a *model validation* phase. The goal was to verify that the visualization and driving sensation during the performance of the drivers closely matched reality, thanks to the use of the Leica BLK 360. Test rides were conducted in the Virtual Reality Laboratory of the Department of Industrial Engineering (Figures 16 and 17). As shown in the figures, they were conducted under sunny conditions as well as cloudy conditions with heavy rain, testing the proper function of the surfaces.ini file, which establishes the tire set's grip parameters. The asphalt temperature was set to stable, and the mobile platform's sensitivity was set to maximum to enhance driving realism as much as possible.



Figure 16. Motion-based driving simulator, Virtual Reality Laboratory, University of Salerno, Department of Industrial Engineering.

Initially, the model failed the tests, showing visual inconsistencies with the real track and errors in reconstructing some track sections, leading to gaps where the car would fall into the void. This initiated an iterative process of error identification, correction, and model validation. This phase was the longest and most complex, as numerous track folder configurations were tested until a solution was found. One error identified was the import scale of the track in Assetto Corsa. Despite the track having the correct dimensions in Blender, it was enlarged by a scale of 100:1 in Assetto Corsa. This generated several functional and visual errors, which were resolved by setting the track export scale from Blender to 1:100 to restore the correct track dimensions.



(**a**) (**b**)

Figure 17. (**a**,**b**) Test rides conducted in the Virtual Reality Laboratory, University of Salerno, Department of Industrial Engineering.

5. Results

The results of the research, focused on utilizing LiDAR technology, demonstrated the effectiveness of this methodology in capturing comprehensive and detailed data points with minimal need for extensive editing and post-production processes. The LiDAR scanner produced an accurate representation of the track, capturing all surface irregularities, such as manholes and bumps, which are critical for creating a realistic driving experience.

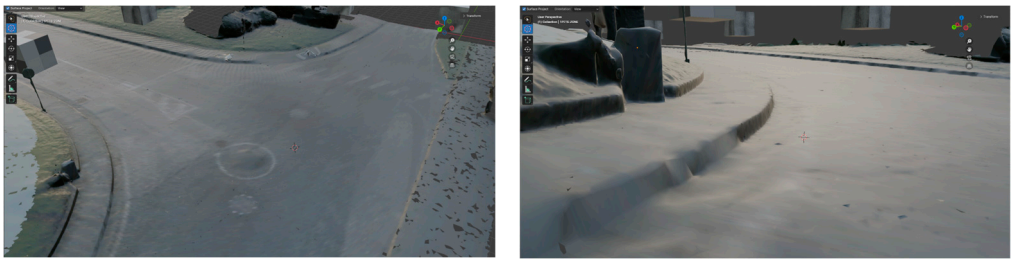
In conclusion, the final construction of the track proved to be highly precise and clean, achieving a point density of approximately 4 mm within a 10 m laser scanning radius and a relatively lower density of 7 mm at a 20 m radius [54]. Every irregularity in the road and sidewalks was measured and seamlessly incorporated into the digital circuit model.

The proposed framework ensured the highest possible fidelity to the real-world scene intended for import into the driving simulation software. In contrast, employing a photogrammetry-based methodology would have yielded considerably lower accuracy, achieving a maximum point density of 20 mm within a 10 m range [38].

Nevertheless, certain challenges arose during the process, including alignment issues that led to point cloud gaps. Despite these limitations, the achieved level of detail and precision far exceeded those of conventional techniques such as photogrammetry. Furthermore, the panoramic and thermographic images captured during the scanning process present promising opportunities for future applications, such as assessing building degradation and analyzing environmental conditions.

In conclusion, the LiDAR acquisition method using the Leica BLK360 is useful and convenient for various reasons. In a few minutes, it is possible to acquire an essential panoramic image for texture creation, avoiding the use of additional devices like drones, thus limiting costs and time for the survey phase [28]; a 360° thermographic image, which, although not useful for the workflow addressed in this approach, could be a great starting point for future developments in analyzing building degradation due to humidity near the track [60]; and an extremely defined and precise point cloud of the surrounding environment. The latter is the most important and distinctive resource of the laser device used. As is shown in Figure 18, the high technology of the scanner is evident in every detail

of the point cloud. The definition and detail complexity of the scans are unparalleled by any other acquisition method used in the modeling field [61].



(**a**) (**b**)

Figure 18. (**a**,**b**) Two sections of the Unisa racetrack—Blender.

It is also noteworthy that a diffuse texture can easily be extracted from the track mesh. By using the appropriate spatial data processing software, such as Agisoft Metashape 2.1.4 it is possible to construct the texture to be associated with the mesh by coloring each polygon present in the model. The color is associated with that from the panoramic images taken by the Leica BLK 360 [58].

6. Conclusions and Future Works

This paper presents a methodology for importing a real-world automotive circuit into the driving simulation software Assetto Corsa v1.16 using LiDAR technology. The data acquisition was conducted with the Leica BLK360 scanner, supported by modeling software employed during the post-production phase. The proposed workflow can be generalized to other case studies beyond automotive circuit modeling, serving as a foundational approach for research in fields such as architecture [62], archeology [63], civil engineering [51], cultural and natural heritage science [64,65], and autonomous vehicles [66], especially considering the ability of the laser scanner to capture thermal point clouds [67].

The study determined that the LiDAR measurement technique, particularly with the use of the Leica BLK360 scanner, offers substantial advantages for the three-dimensional modeling of tracks in simulated driving environments. The technique provides a detailed polygonal grid with minimal post-processing requirements, setting it apart from other methods that necessitate extensive editing [34]. However, such high precision in detail requires very powerful computers and modeling software, which are not accessible to all users. In scenarios where extreme precision is not essential, simplifications can be applied to reduce the size of the point cloud. In this case, the point cloud should be corrected by applying a series of simplifications through Agisoft Metashape. For the mesh reconstruction, simplifications for approximately 1 km of track would have resulted in reducing the point cloud from 734,155,511 vertices (Figure 19) to 36,056,681 vertices, which is 5% of the total points.

In addition to the positive aspects, the use of the LiDAR methodology also presented some limitations. First, during the survey phase, the Leica BLK360 needed to remain stationary for about 3 min, and having to perform scans on an open road sometimes caused problems with the passage of cars or people, partially compromising the survey and slowing down the work. Specifically, the Leica BLK360 is very sensitive to high temperatures [54] and, as mentioned earlier in the case study, this reduced battery life. Finally, the Leica Cyclone Register Plus 360 v2023.1.0 software, although rapid and effective for scan alignment, lacks other functionalities useful for modeling. A solution could be to use another Leica software package, such as Leica Cyclone 3DR, which, unlike Cyclone Register Plus 360, allows the obtainment of more information from the point cloud and

building of a classified mesh [68–70]. It is not possible to decode the scans, as they are in .blk format (Leica proprietary), in non-Leica proprietary software.



Figure 19. Point count—Leica Cyclone Register 360 Plus.

Unlike photogrammetry, the road model was much more complex and elaborate, capturing every road inclination and irregularity. Photogrammetry performed using, for example, a GoPro camera and a drone for aerial shots would have required a budget of a few thousand euros [28]. However, it is essential to note that the achievable result is significantly less performant than that obtained with a laser scanner. Additionally, achieving comparable outcomes would have required considerably more extensive scanning efforts and post-production work, further increasing the complexity and time demands of the process [61].

Despite some limitations, such as the scanner's sensitivity to high temperatures and the need for it to remain stationary during scans, the LiDAR method, using the Leica BLK360, proves to be superior in capturing the topographical features of road surfaces [61]. These detailed data are crucial for creating realistic and immersive virtual driving simulations, bridging the gap between real-world and simulated environments [38].

Future improvements and developments in this field could focus on several areas to enhance the accuracy and usability of the 3D models created from LiDAR data. As this is the first project of 3D modeling of a real track for import into a driving simulation software package using the LiDAR method, it is evident that there is a high margin for improvement. The alignment of the scans could first be optimized by overlaying points from the drone [28]. This could also further define the texture of the model, providing additional visual information to the entire map. Therefore, it may be advisable to consider incorporating points obtained from photogrammetry to further refine the scenario [71]. Alternatively, an association mechanism could be introduced to facilitate information exchange between LiDAR point clouds and meshes, enhancing the integration and improving the overall accuracy of the reconstructed model [72].

During the workflow, another critical aspect was the cleaning of scans to remove unwanted elements such as people, vehicles, and objects. This challenge could be addressed through the integration of advanced tools capable of identifying and removing noise within the scans without compromising the integrity of the entire point cloud [73,74].

Another improvement could come from more detailed modeling of natural objects, such as trees and hedges, which in this work was not essential for track modeling as the goal was to define the road and adjacent sidewalks as precisely as possible.

Moreover, given the current technologies, one could also model a three-dimensional space using a NeRF, which allows, through artificial intelligence, modeling of a 3D scenario from 2D information, thus further automating the process of transitioning from the physical world to the virtual reality of the driving simulator. A NeRF, or neural radiance field, is an artificial intelligence model that takes 2D images representing a scene as input and interpolates them to render a complete 3D scene. The model functions as a neural network,

a model that replicates the organization of the brain and is often used for tasks requiring pattern recognition [75,76]. This technology could streamline the modeling process, making it more accessible and efficient.

Finally, it would also be possible to utilize the thermal camera features integrated into the Leica BLK 360 [77,78]. This functionality could be applied to measure the surface temperature of buildings [67,79], enabling the analysis of moisture levels in the walls of structures adjacent to the road [60]. Such an approach could facilitate studies on climatic effects on the buildings of the University of Salerno, providing valuable insights into environmental impacts and structural health.

Beyond driving simulators, the methodologies developed in this study could be applied to other fields requiring precise 3D modeling, such as urban planning, architecture, and environmental studies [65,80].

These future developments hold the potential to significantly enhance the transition from physical environments to virtual driving simulators, providing users with more accurate, detailed, and immersive experiences. As technology continues to advance, the integration of these improvements could lead to new standards in the field of virtual reality and simulation.

Author Contributions: All authors equally contributed to carrying out the research, whose results are reported in this work. All authors have read and agreed to the published version of the manuscript.

Funding: This research received no external funding.

Data Availability Statement: The original contributions presented in this study are included in the article. Further inquiries can be directed to the corresponding authors.

Conflicts of Interest: The authors declare no conflicts of interest.

References

1. Colditz, J.; Dragon, L.; Faul, R.; Meljnikov, D.; Schill, V.; Unselt, T.; Zeeb, E. Use of Driving Simulators Within Car Development. 2007. Available online: https://www.nads-sc.uiowa.edu/dscna/2007/papers/Section%202B%20-%20Simulator%20Characteristics%20-%20Applications%20I/Zeeb.pdf (accessed on 20 April 2024).
2. Professor, A.; Messina, M. Potentialities of Driving Simulator for Engineering Applications to Formula 1. Available online: https://cdn.archilovers.com/projects/39c6eb1a-29fb-4e19-8112-736fcb14ab84.pdf (accessed on 1 September 2024).
3. de Winter, J.C.F.; de Groot, S.; Mulder, M.; Wieringa, P.A.; Dankelman, J.; Mulder, J.A. Relationships between Driving Simulator Performance and Driving Test Results. *Ergonomics* **2009**, *52*, 137–153. [CrossRef] [PubMed]
4. Yan, X.; Abdel-Aty, M.; Radwan, E.; Wang, X.; Chilakapati, P. Validating a Driving Simulator Using Surrogate Safety Measures. *Accid. Anal. Prev.* **2008**, *40*, 274–288. [CrossRef] [PubMed]
5. Godley, S.T.; Triggs, T.J.; Fildes, B.N. Driving Simulator Validation for Speed Research. *Accid. Anal. Prev.* **2002**, *34*, 589–600. [CrossRef]
6. Mourão, P. *The economics of Motorsports: The Case of Formula One*; Springer: Berlin/Heidelberg, Germany, 2017.
7. Haugen, S.; Barros, A.; van Gulijk, C.; Kongsvik, T.; Vinnem, J.E. *Simulator Training in Driver Education-Potential Gains and Challenges-Safety and Reliability: Safe Societies in a Changing World: Proceedings of the 28th International European Safety and Reliability Conference (ESREL 2018), Trondheim, Norway, 17–21 June 2018*; Taylor & Francis Group: London, UK; Trondheim, Norway, 2018; ISBN 9780815386827.
8. Khusro, Y.R.; Zheng, Y.; Grottoli, M.; Shyrokau, B. MPC-Based Motion-Cueing Algorithm for a 6-DOF Driving Simulator with Actuator Constraints. *Vehicles* **2020**, *2*, 625–647. [CrossRef]
9. Park, G.D.; Allen, R.W.; Rosenthal, T.J.; Fiorentino, D. Training effectiveness: How does driving simulator fidelity influence driver performance? In *Proceedings of the Human Factors and Ergonomics Society Annual Meeting*; SAGE Publications: Hawthorne, CA, USA, 2005; Voloume 49, pp. 2201–2205.
10. Damian, S.; Pradeep, R.; Amir, T.-K.; Jitendra, J.; Suchada, V. Assessing Video Games to Improve Driving Skills: A Literature Review and Observational Study. *JMIR Serious Games* **2014**, *2*, e5. [CrossRef]
11. Bruck, L.; Haycock, B.; Emadi, A. A Review of Driving Simulation Technology and Applications. *IEEE Open J. Veh. Technol.* **2021**, *2*, 1–16. [CrossRef]

12. Fisher, D.L.; Caird, J.K.; Rizzo, M.; Lee, J.D. *Handbook of Driving Simul Ation for Engineering, Medicine, and Psychology*; CRC Press: Boca Raton, FL, USA, 2011.
13. Aykent, B.; Merienne, F.; Guillet, C.; Paillot, D.; Kemeny, A. Motion Sickness Evaluation and Comparison for a Static Driving Simulator and a Dynamic Driving Simulator. *Proc. Inst. Mech. Eng. Part D J. Automob. Eng.* **2014**, *228*, 818–829. [CrossRef]
14. Zhou, H.P.; Itoh, M.; Kitazaki, S. Effect of Instructing System Limitations on the Intervening Behavior of Drivers in Partial Driving Automation. *Cogn. Technol. Work* **2020**, *22*, 321–334. [CrossRef]
15. Mourant, R.R.; Sadhu, P. Evaluation of force feedback steering in a fixed based driving simulator. *Proc. Hum. Factors Ergon. Soc. Annu. Meet.* **2002**, *46*, 2202–2205. [CrossRef]
16. Vinattieri, F.; Morrocchi, L.; Capitani, R.; Annicchiarico, C. Sviluppo di un'apparecchiatura sperimentale per l'integrazione del sistema di sterzo in un simulatore di statico. In *Convegno Nazionale Associazione Italiana per l'Analisi delle Sollecitazioni*; Associazione Italiana per l'Analisi delle Sollecitazioni: Rome, Italy, 2017; pp. 1–12.
17. Barlocco, I.S.; Preiti, D.; Mastinu, G. School of Industrial and Information Engineering Optimisation of the Tyre Model in RFactor2 Environment for AVEHIL Professional Simulator; Milano 2018. Available online: https://www.politesi.polimi.it/retrieve/a81cb05d-9cd9-616b-e053-1605fe0a889a/Optimisation%20of%20the%20tyre%20model%20in%20rFactor2%20environment%20for%20AVEHIL%20professional%20simulator.pdf (accessed on 21 April 2024).
18. 3DOS Motion System. Available online: https://zs3dof.jimdofree.com/ (accessed on 21 April 2024).
19. Klüver, M.; Herrigel, C.; Heinrich, C.; Schöner, H.P.; Hecht, H. The Behavioral Validity of Dual-Task Driving Performance in Fixed and Moving Base Driving Simulators. *Transp. Res. Part F Traffic. Psychol. Behav.* **2016**, *37*, 78–96. [CrossRef]
20. Casillo, M.; Cecere, L.; Colace, F.; Lombardi, M.; Lorusso, A.; Santoriello, A. Serious Gaming for Cultural Heritage: The Case Study of the Domus of Abellinum. In *International Congress on Information and Communication Technology*; Springer Nature: Singapore, 2024; pp. 203–214.
21. Cecere, L.; Colace, F.; Lorusso, A.; Santaniello, D. Predictive Maintenance of an Archeological Park: An IoT and Digital Twin Based Approach. In *International Conference on Human-Computer Interaction*; Springer Nature: Cham, Switzerland, 2024; pp. 323–341.
22. Barba, S.; Villecco, F.; Naddeo, A. "Ultima Dea": A Laser Scanner Application for 3D Modelling. In *Advances in Intelligent Systems and Computing*; Springer: Cham, Switzerland, 2019; Volume 809, pp. 559–569.
23. Li, Y.; Ibanez-Guzman, J. Lidar for Autonomous Driving: The Principles, Challenges, and Trends for Automotive Lidar and Perception Systems. *IEEE Signal Process. Mag.* **2020**, *37*, 50–61. [CrossRef]
24. Bosello, M.; Tse, R.; Pau, G. Train in Austria, Race in Montecarlo: Generalized RL for Cross-Track F1tenthLIDAR-Based Races. In Proceedings of the 2022 IEEE 19th Annual Consumer Communications & Networking Conference (CCNC), Las Vegas, NV, USA, 8–11 January 2022; Institute of Electrical and Electronics Engineers Inc.: New York, NY, USA, 2022; pp. 290–298.
25. Linkov, V.; Zámečník, P.; Zaoral, A. The Use of Driving Simulators in Psychological Research. *Sib. Psikhologicheskiy Zhurnal* **2017**, *64*, 65–75. [CrossRef]
26. Plumley, D.; Wilson, R. *The Economics and Finance of Professional Team Sports*; Routledge: London, UK, 2022.
27. Dorn, L.; Barker, D. The effects of driver training on simulated driving performance. *Accid. Anal. Prev.* **2005**, *37*, 63–69. [CrossRef] [PubMed]
28. Morer Camo, P.; Medina, A. Low-Cost 3D modelling to integrate an existing karting circuit into a simulator using aerial photogrammetry with drones. *Dyna* **2021**, *96*, 73–78. [CrossRef] [PubMed]
29. Kirsten, E.; Inocencio, L.C.; Veronez, M.R.; Da Silveira, L.G.; Bordin, F.; Marson, F.P. 3D Data Acquisition Using Stereo Camera. In Proceedings of the IGARSS 2018-2018 IEEE International Geoscience and Remote Sensing Symposium, Valencia, Spain, 22–27 July 2018; IEEE: Piscataway, NJ, USA, 2018. ISBN 9781538671504.
30. Cleveland, L.J.; Wartman, J. Principles and Applications of Digital Photogrammetry for Geotechnical Engineering. In Proceedings of the Site and Geomaterial Characterization, Shanghai, China, 6–8 June 2006; American Society of Civil Engineers: Reston, VA, USA, 2006; pp. 128–135.
31. di Filippo, A.; Antinozzi, S.; Cappetti, N.; Villecco, F. Methodologies for Assessing the Quality of 3D Models Obtained Using Close-Range Photogrammetry. *Int. J. Interact. Des. Manuf.* **2024**, *18*, 5917–5924. [CrossRef]
32. di Filippo, A.; Villecco, F.; Cappetti, N.; Barba, S. A Methodological Proposal for the Comparison of 3D Photogrammetric Models. In *Design Tools and Methods in Industrial Engineering II*; Lecture Notes in Mechanical Engineering; Springer: Cham, Switzerland, 2022; pp. 930–937.
33. Gomarasca, M.A. Basics of Geomatics. *Appl. Geomat.* **2010**, *2*, 137–146. [CrossRef]
34. Deliry, S.I.; Avdan, U. Accuracy of Unmanned Aerial Systems Photogrammetry and Structure from Motion in Surveying and Mapping: A Review. *J. Indian Soc. Remote Sens.* **2021**, *49*, 1997–2017. [CrossRef]
35. Moyano, J.; Nieto-Julián, J.E.; Bienvenido-Huertas, D.; Marín-García, D. Validation of Close-Range Photogrammetry for Architectural and Archaeological Heritage: Analysis of Point Density and 3d Mesh Geometry. *Remote Sens.* **2020**, *12*, 3571. [CrossRef]

36. Casillo, M.; Colace, F.; Gupta, B.B.; Lorusso, A.; Marongiu, F.; Santaniello, D. A Deep Learning Approach to Protecting Cultural Heritage Buildings Through IoT-Based Systems. In Proceedings of the 2022 IEEE International Conference on Smart Computing (SMARTCOMP), Helsinki, Finland, 20–24 June 2022; Institute of Electrical and Electronics Engineers Inc.: Piscataway, NJ, USA, 2022; pp. 252–256.
37. Marín-Buzón, C.; Pérez-Romero, A.; López-Castro, J.L.; Ben Jerbania, I.; Manzano-Agugliaro, F. Photogrammetry as a New Scientific Tool in Archaeology: Worldwide Research Trends. *Sustainability* **2021**, *13*, 5319. [CrossRef]
38. Sapirstein, P. Accurate Measurement with Photogrammetry at Large Sites. *J. Archaeol. Sci.* **2016**, *66*, 137–145. [CrossRef]
39. Antinozzi, S.; di Filippo, A.; Morena, S.; Sanseverino, A.; Villecco, F. Prototyping a Mechanical Mounting System for the Photogrammetric Use of USB Microscopes. In *Design Tools and Methods in Industrial Engineering III*; Carfagni, M., Furferi, R., Di Stefano, P., Governi, L., Gherardini, F., Eds.; Springer: Cham, Switzerland, 2024; pp. 66–76.
40. Fang, K.; Zhang, J.; Tang, H.; Hu, X.; Yuan, H.; Wang, X.; An, P.; Ding, B. A Quick and Low-Cost Smartphone Photogrammetry Method for Obtaining 3D Particle Size and Shape. *Eng. Geol.* **2023**, *322*, 107170. [CrossRef]
41. Hu, C.; Kong, L.; Lv, F. Application of 3D Laser Scanning Technology in Engineering Field. *E3S Web Conf.* **2021**, *233*, 04014. [CrossRef]
42. Risse, B.; Mangan, M.; Stürzl, W.; Webb, B. Software to Convert Terrestrial LiDAR Scans of Natural Environments into Photorealistic Meshes. *Environ. Model. Softw.* **2018**, *99*, 88–100. [CrossRef]
43. Liu, B.; Yu, Y.; Jiang, S. Review of Advances in LiDAR Detection and 3D Imaging. *Guangdian Gongcheng/Opto-Electron. Eng.* **2019**, *46*, 190167.
44. Raj, T.; Hashim, F.H.; Huddin, A.B.; Ibrahim, M.F.; Hussain, A. A Survey on LiDAR Scanning Mechanisms. *Electronics* **2020**, *9*, 741. [CrossRef]
45. A. M. Assetto Corsa Modding Manual 3.0. 2023. Available online: https://www.scribd.com/document/700457509/Assetto-Corsa-Modding-Manual-3-0-0-27revh (accessed on 1 September 2024).
46. Wang, R.; Peethambaran, J.; Chen, D. LiDAR Point Clouds to 3-D Urban Models: A Review. *IEEE J. Sel. Top Appl. Earth Obs. Remote Sens.* **2018**, *11*, 606–627. [CrossRef]
47. Santos, B.; Rodrigues, N.; Costa, P.; Coelho, A. Integration of CAD Models into Game Engines. In Proceedings of the VISIGRAPP 2021—Proceedings of the 16th International Joint Conference on Computer Vision, Imaging and Computer Graphics Theory and Applications, Virtual Event, 8–10 February 2021; SciTePress: Setúbal, Portugal, 2021; Volume 1, pp. 153–160.
48. Siljedahl, R.; Eles, P. 3D Conversion from CAD Models to Polygon Models. 2016. Available online: https://www.diva-portal.org/smash/record.jsf?pid=diva2:944914&dswid=-5337 (accessed on 15 September 2024).
49. Ostrovka, D.; Teslyuk, V. The Analysis of File Format Conversion Tools for Storing 3D Objects for the IOS Platform. 2020. Available online: https://ceur-ws.org/Vol-2631/paper26.pdf (accessed on 15 September 2024).
50. Gries, D.; Schneider, F.B. *The Computer Graphics Manual*; Springer Science & Business Media: Berlin/Heidelberg, Germany, 2011.
51. International Network of Mechatronics Universities; Higher Technological Institute; Institute of Electrical and Electronics Engineers. A Modular Architecture of a PC-Based Driving for Advanced Driver Assistance Systems. In Proceedings of the 15th International Workshop on Research and Education in Mechatronics (REM), El Gouna, Egypt, 9–11 September 2014; ISBN 9781479930296.
52. Institute of Electrical and Electronics Engineers. Modeling virtual driving environment for a driving simulator. In Proceedings of the 2011 IEEE International Conference on Control System, Computing and Engineering, ICCSCE 2011, Batu Ferringhi, Malaysia, 25–27 November 2011; IEEE: Piscataway, NJ, USA, 2011. ISBN 9781457716423.
53. Kemeny, A. From Driving Simulation to Virtual Reality. In Proceedings of the 2014 Virtual Reality International Conference, Laval, France, 9–11 April 2014.
54. Leica BLK360 User Manual. 2020. Available online: https://shop.leica-geosystems.com/sites/default/files/2022-01/853811_Leica_BLK360_UM_v4.0.0_en.pdf (accessed on 1 April 2024).
55. Li, N.; Ho, C.P.; Xue, J.; Lim, L.W.; Chen, G.; Fu, Y.H.; Lee, L.Y.T. A Progress Review on Solid-State LiDAR and Nanophotonics-Based LiDAR Sensors. *Laser Photon Rev.* **2022**, *16*, 2100511. [CrossRef]
56. Thomas, H. Some like It Hot: The Impact of next Generation FLIR Systems Thermal Cameras on Archaeological Thermography. *Archaeol Prospect* **2018**, *25*, 81–87. [CrossRef]
57. Leica_Cyclone_REGISTER_360_QuickStartGuide_BLK_Edition. Leica GeoSystems 2024. Available online: https://shop.leica-geosystems.com/sites/default/files/2022-06/Leica_Cyclone_REGISTER_360_QuickStartGuide_BLK_Edition.pdf (accessed on 2 April 2024).
58. *Agisoft Metashape User Manual Professional Edition, Version 2.1*; Agisoft LLC.: St. Petersburg, Russia, 2024.
59. Huang, C. *Mathematical Characterization of Road Surface Texture and Its Relation to Laboratory Friction Measures*; Michigan Technological University: Houghton, MI, USA, 2003.
60. Kaartinen, E.; Dunphy, K.; Sadhu, A. LiDAR-Based Structural Health Monitoring: Applications in Civil Infrastructure Systems. *Sensors* **2022**, *22*, 4610. [CrossRef]

61. Abreu, N.; Pinto, A.; Matos, A.; Pires, M. Procedural Point Cloud Modelling in Scan-to-BIM and Scan-vs-BIM Applications: A Review. *ISPRS Int. J. Geoinf.* **2023**, *12*, 260. [CrossRef]
62. Calisi, D.; Botta, S.; Cannata, A. Integrated Surveying, from Laser Scanning to UAV Systems, for Detailed Documentation of Architectural and Archeological Heritage. *Drones* **2023**, *7*, 568. [CrossRef]
63. Balan, M.; Majecki, P.; Grimble, M.; Blackwell, P. Multiple degrees of freedom active motion control of a hydraulically actuated crane. In Proceedings of the OCEANS 2021, San Diego, CA, USA, 20–23 September 2021; IEEE: Piscataway, NJ, USA, 2021; ISBN 9780692935590.
64. Del Duca, G.; Machado, C. Assessing the Quality of the Leica BLK2GO Mobile Laser Scanner versus the Focus 3D S120 Static Terrestrial Laser Scanner for a Preliminary Study of Garden Digital Surveying. *Heritage* **2023**, *6*, 1007–1027. [CrossRef]
65. Gril, E.; Laslier, M.; Gallet-Moron, E.; Durrieu, S.; Spicher, F.; Le Roux, V.; Brasseur, B.; Haesen, S.; Van Meerbeek, K.; Decocq, G.; et al. Using Airborne LiDAR to Map Forest Microclimate Temperature Buffering or Amplification. *Remote Sens. Environ.* **2023**, *298*, 113820. [CrossRef]
66. Sammartano, G.; Spreafico, A.; Tanduo, B.; Chiabrando, F. Robotics for Heritage Surveying: Preliminary Test on Leica BLK ARC & Spot® toward Autonomous 3D Mapping. *Int. Arch. Photogramm. Remote Sens. Spat. Inf. Sci.* **2024**, *48*, 579–586.
67. Borrmann, D.; Nüchter, A.; Đakulović, M.; Maurović, I.; Petrović, I.; Osmanković, D.; Velagić, J. A Mobile Robot Based System for Fully Automated Thermal 3D Mapping. *Adv. Eng. Inform.* **2014**, *28*, 425–440. [CrossRef]
68. Fahlander, F.; Axelsson, T. The Rock, the Whole Rock, and Everything about the Rock. *Situ Archaeol.* **2023**, *16*, 49–66. [CrossRef]
69. Kovanič, Ľ.; Blišťan, P.; Topitzer, B.; Peťovský, P.; Boczek, R. TLS and low-cost UAV photogrammetry as an effective combination of spatial data collection methods for creating detailed 3D surface models (DEM). *GIS Odyssey J.* **2023**, *3*, 163–178. [CrossRef]
70. Chiominto, L.; D'Emilia, G.; Marsella, S.; Marzoli, M.; Natale, E. Point Cloud Processing Methods for Slope Analysis: Uncertainty Evaluation. In Proceedings of the 2024 IEEE International Workshop on Metrology for Living Environment (MetroLivEnv), Chania, Greece, 12–14 June 2024; Institute of Electrical and Electronics Engineers Inc.: Piscataway, NJ, USA, 2024; pp. 156–160.
71. Kudela, P.; Palčák, M.; Zábovská, K.; Bučko, B. Integration of photogrammetry within laser scanning approach. In Proceedings of the 2020 43rd International Convention on Information, Communication and Electronic Technology (MIPRO), Opatija, Croatia, 28 September–2 October 2020.
72. Laupheimer, D.; Shams Eddin, M.H.; Haala, N. On the Association of Lidar Point Clouds and Textured Meshes for Multi-Modal Semantic Segmentation. *ISPRS Ann. Photogramm. Remote Sens. Spat. Inf. Sci.* **2020**, *2*, 509–516. [CrossRef]
73. Pepe, M.; Garofalo, A.R.; Costantino, D.; Tana, F.F.; Palumbo, D.; Alfio, V.S.; Spacone, E. From Point Cloud to BIM: A New Method Based on Efficient Point Cloud Simplification by Geometric Feature Analysis and Building Parametric Objects in Rhinoceros/Grasshopper Software. *Remote Sens.* **2024**, *16*, 1630. [CrossRef]
74. Nunes, L.; Marcuzzi, R.; Mersch, B.; Behley, J.; Stachniss, C. Scaling Diffusion Models to Real-World 3D LiDAR Scene Completion. In Proceedings of the IEEE/CVF Conference on Computer Vision and Pattern Recognition (CVPR), Seattle, WA, USA, 16–22 June 2024.
75. Ghadekar, P.; Gonepuri, A.; Deshpande, P.; Dhole, V.; Dharwadkar, M.; Sonkamble, P.; Saraf, C. Generating 3D Models for Prototyping of Virtual Environments Using NeRF. In Proceedings of the 2024 Second International Conference on Emerging Trends in Information Technology and Engineering (ICETITE), Vellore, India, 22–23 February 2024. [CrossRef]
76. Remondino, F.; Karami, A.; Yan, Z.; Mazzacca, G.; Rigon, S.; Qin, R. A Critical Analysis of NeRF-Based 3D Reconstruction. *Remote Sens.* **2023**, *15*, 3585. [CrossRef]
77. Zhu, J.; Xu, Y.; Ye, Z.; Hoegner, L.; Stilla, U. Fusion of Urban 3D Point Clouds with Thermal Attributes Using MLS Data and TIR Image Sequences. *Infrared Phys. Technol.* **2021**, *113*, 103622. [CrossRef]
78. Niskanen, I.; Duan, G.; Vartiainen, E.; Immonen, M.; Hallman, L.; Kostamovaara, J.; Heikkilä, R. Enhancing Point Cloud Data Fusion through 2D Thermal Infrared Camera and 2D Lidar Scanning. *Infrared Phys. Technol.* **2024**, *141*, 105432. [CrossRef]
79. Adán, A.; López-Rey, A.; Ramón, A. Robot for Thermal Monitoring of Buildings. *Autom. Constr.* **2023**, *154*, 105009. [CrossRef]
80. Chajaei, F.; Bagheri, H. Machine Learning Framework for High-Resolution Air Temperature Downscaling Using LiDAR-Derived Urban Morphological Features. *Urban Clim.* **2024**, *57*, 102102. [CrossRef]

Disclaimer/Publisher's Note: The statements, opinions and data contained in all publications are solely those of the individual author(s) and contributor(s) and not of MDPI and/or the editor(s). MDPI and/or the editor(s) disclaim responsibility for any injury to people or property resulting from any ideas, methods, instructions or products referred to in the content.